Available online at www.sciencedirect.com
ScienceDirect
Journal of Catalysis 252 (2007) 148–160
JOURNAL OF CATALYSIS
www.elsevier.com/locate/jcat

Activation and reactivity of epoxides on solid acid catalysts

L. Saikia, J.K. Satyarthi, D. Srinivas *, P. Ratnasamy *

National Chemical Laboratory, Pune 411 008, India

Received 24 July 2007; revised 28 September 2007; accepted 2 October 2007

Abstract

The aminolysis of epoxides over novel solid catalysts (Brönsted-acidic SBA-15 functionalized with propylsulfonic acid and Lewis-acidic Ti-MCM-41) is reported. The acidic properties of these catalysts were determined by FTIR spectroscopy and temperature-programmed desorption of pyridine and NH_3, respectively. The mesoporous solid acids of the present study are reusable and exhibit significantly higher catalytic activities than known catalysts for opening of the oxirane ring with nitrogen (aromatic and aliphatic amines)-containing and oxygen (alcohols)-containing nucleophiles. A range of β-amino alcohols with high regioselectivity and stereoselectivity were synthesized. Adsorption studies as well as the sigmoid shape of the conversion-versus-time plots show that the epoxide and amine compete for adsorption on the acidic sites ($-SO_3H$ or Ti^{4+}) on the catalyst surface. Epoxide adsorption and activation on acid sites are the more critical processes. Catalytic activity decreases with increasing basicity of the amines and/or the alcohol, as well as the dielectric constant of the solvent.

Keywords: SBA-15 functionalized with propylsulfonic acid; Ti-MCM-41; Solid acids; Aminolysis and alcoholysis of epoxides; β-Amino alcohols; Ring opening of epoxides

1. Introduction

Epoxides are versatile and important intermediates in pharmaceutical and agrochemical industries. The three-membered heterocyclic ring is strained and offers an uncommon combination of reactivity, synthetic flexibility, and atom economy. It is susceptible to attack by a range of nucleophiles, including nitrogen (e.g., ammonia, amines, azides), oxygen (e.g., water, alcohols, phenols, acids), and sulfur (thiol)-containing compounds, leading to bifunctional molecules of great industrial value. For example, β-amino alcohols (Scheme 1) are used in the synthesis of β-blockers, insecticidal agents, and oxazolines and as chiral ligands in asymmetric synthesis [1–5]. The classical synthesis of β-amino alcohol involves the ring opening of epoxides with amines. These reactions are conventionally carried out with a large excess of the amines at elevated temperatures and in the presence of solvents. This method is less effective for weakly nucleophilic amines and yields low regioselectivity [6,7]. Various catalyst systems, including sulfamic acid, amberlyst resin, metal triflates, transition metal halides, ionic liquids, zeolites, and Lewis acids, in a supercritical carbon dioxide medium have been investigated [8–15]. All of these catalysts necessitate long reaction times, elevated temperatures, high pressures, stoichiometric amounts of catalyst, and use of expensive reagents or catalysts. Recently, the ring opening of epoxides in water in the absence of any catalyst was reported, but this required a long reaction time, and the product yield was low [16]. Even though heterogeneous catalysts have been used in the ring-opening addition of such nucleophiles as amines and alcohols to epoxides, their activity and selectivity also have been low. For example, Garcia et al. [17] reported that in the reaction between styrene epoxide and *n*-propanol, zeolite Y gave conversions only in the range of 5–10%, and many secondary products were formed. Robinson et al. [18] reported that mesoporous aluminosilicates catalyzed the alcoholysis of epoxides to give β-alkoxyalcohols in high yields at room temperature in short reaction times (1–4.5 h). Recently, we reported preliminary results on the aminolysis of

* Corresponding authors. Fax: +91 20 2590 2633.
E-mail addresses: d.srinivas@ncl.res.in (D. Srinivas), p.ratnasamy@ncl.res.in (P. Ratnasamy).

0021-9517/$ – see front matter
doi:10.1016/j.jcat.2007.10.002

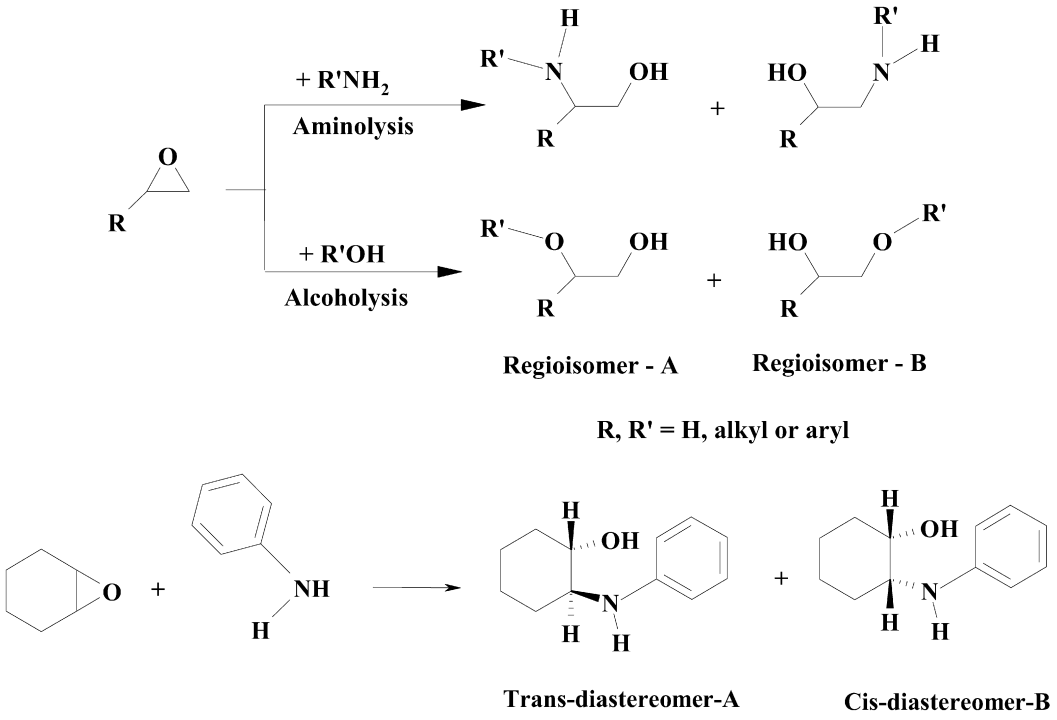

Scheme 1. Reactions of epoxides with nucleophiles.

epoxides over Lewis-acidic titanosilicates [19]. In the present report, we present more detailed information on this system and compare its activity and selectivity with that of a solid Brönsted acid (sulfonic acid-functionalized SBA-15) in this reaction.

Sulfonic acid-functionalized mesoporous silica [20,21] has been used as a catalyst for the esterification of carboxylic acid with alcohols [22–24], the synthesis of polycaprolactone [25], and oxidation reactions [26,27]. Titanosilicate molecular sieves (TS-1 and Ti-MCM-41) have long been known to have remarkable selective oxidation activity of organic molecules at mild conditions using H_2O_2 as an oxidant [28,29]. We have reported on their novel application as solid catalysts for the synthesis of polycarbonate and polyurethane precursors using CO_2 instead of toxic phosgene [30–33] and for transesterification reactions of carbonates and carboxylic acid esters [30,34]. Garro et al. [35] were the first to report their use as a solid Lewis acid in Mukaiyama-type aldol condensation reactions.

The aims of the present study are (1) to compare the activity and especially the selectivity of the solid Lewis (titanosilicates) and Brönsted (sulfonated SBA-15) acids for the aminolysis of epoxides, and (2) to delineate the dominant structural, adsorption, and other kinetic parameters that control the rates and selectivity in this reaction. In contrast to the alcoholysis of epoxides, not much information is available on the use of solid Lewis or Brönsted acids for the aminolysis of epoxides. A range of β-amino and alkoxy alcohols were synthesized using these solid catalysts in very high yields from symmetrical and unsymmetrical epoxides (with aromatic and aliphatic amines/alcohols) at ambient temperatures and under solvent-free conditions.

2. Experimental

2.1. Material preparation

SBA-15 was prepared [36] using tetraethyl orthosilicate (TEOS, Aldrich) as the silica source, poly(ethylene glycol)-block-poly(propylene glycol)-block-poly(ethylene glycol) (Pluronic P123, $EO_{20}PO_{70}EO_{20}$, average molecular weight = 5800, Aldrich) as the template, and HCl as the pH controlling agent. 3-Mercaptopropyltrimethoxysilane (MPTMS) was procured from Aldrich. All of the solvents and chemicals were of A.R. grade and purchased from Merck India Ltd.

2.1.1. Preparation of SBA-15 functionalized with propylthiol

Propylthiol functionalization was accomplished by condensing the surface silanol groups of SBA-15 with MPTMS [37–39]. In a typical preparation, calcined SBA-15 (4 g) was first activated under vacuum at 423 K for 4 h, then dispersed in dry toluene (100 mL). Then 5.42 g of MPTMS was added to it, in small amounts over 10 min. The contents of the flask were refluxed under nitrogen for 24 h. Soxhlet extraction, first with dichloromethane for 12 h and then with acetone for 12 h, yielded the thiol-functionalized SBA-15 (SBA-15-*pr*-SH). This was dried at 353 K. The thiol loading estimated by sulfur analysis was 1.5 mmol/g.

2.1.2. Preparation of SBA-15 functionalized with propylsulfonic acid

To 4 g of SBA-15-*pr*-SH (activated at 373 K) was added 65 mL of 30% aq. H_2O_2 [40–42]. The mixture was then stirred for 8 h at 298 K. The solid was filtered, washed with deionized water and dried, first at 298 K for 24 h and then at 353 K

Table 1
Chemical composition and structural properties of functionalized SBA-15 materials

System	Elemental analysis (wt%)			Organic functional group (mmol/g)[a]	XRD		N_2 adsorption				Wall thickness (nm)
	C	H	S		d_{100} (nm)	Unit cell parameter (nm)	Pore diameter (nm)	Specific surface area (m^2/g)		Total pore volume (cm^3/g)	
								BET	BJH		
SBA-15	0.4	0.9	0	0	9.5	11.0	6.5	692	686	1.13	4.5
SBA-15-*pr*-SH	6.3	1.8	4.7	1.5 (1.7)	9.9	11.5	6.5	534	554	0.87	5.0
SBA-15-*pr*-SO_3H	4.8	1.8	1.8	0.6 (0.7)	9.7	11.3	6.2	533	546	0.83	5.1

[a] Determined from the S-content. Values in parentheses are those estimated from the thermo-gravimetric analysis data.

for 12 h, to obtain propylsulfonic acid-functionalized SBA-15 (SBA-15-*pr*-SO_3H). Based on the elemental sulfur analysis, the content of the -*pr*-SO_3H functional group in this material was 0.6 mmol/g silica (Table 1). The acidity/ion exchange capacity of the catalyst was estimated as 0.73 mEq/g silica. This estimation by the titrimetric method agrees well with that obtained from the sulfur analysis (Table 1).

2.1.3. Preparation of titanosilicate molecular sieves

TS-1 (Si/Ti = 33; $S_{BET} = 485\ m^2/g$) was synthesized as described previously [43]. In a typical synthesis of Ti-MCM-41 (input ratio of Si/Ti = 30), 2.67 g of sodium hydroxide was dissolved in 147 g of distilled water. To this, 5.94 g of cetyltrimethylammonium bromide (CTMABr, S.D. Fine Chemicals Ltd., India) was added. Then 4 g of fumed silica (Aldrich) was added slowly under stirring over 45 min. The stirring was continued for another 1 h, with the pH of the gel maintained at 9–10 using dilute H_2SO_4 solution. To this was added 0.657 g of titanium isopropoxide (Aldrich) in 5–10 mL of iso-propanol over 15 min. The resulting gel was stirred for another 5 h at 298 K, then transferred into a Teflon-lined stainless steel autoclave and heated to 373 K for 48 h. The solid product was filtered, washed with distilled water, dried at 353 K, and finally calcined at 813 K for 6 h. The output Si/Ti ratio was found to be 35.

2.2. Characterization techniques

X-ray diffraction (XRD) was performed with a Philips X'Pert Pro diffractometer using Cu$K\alpha$ radiation and a proportional counter as a detector. Morphological characteristics of the samples were determined by scanning electron microscopy (SEM) using a Leica 440 microscope and transmission electron microscopy (TEM) using a JEOL 1200EX microscope operating at 100 kV. Elemental analyses (C, H, and S) of the samples were performed using a Carlo-Erba 1106 analyzer. The specific surface areas (BET) of the samples were determined using a Quanta Chrome NOVA 1200 instrument. The data points of p/p_0 in the range of ca. 0.05–0.3 were used in the calculations. The micropore volume was estimated from the t-plot, and the pore diameter was estimated using the BJH model. Thermogravimetric analysis was done on a Seiko DTA-TG 320 instrument under air (50 mL/min), at a ramp rate of 10 K/min, in the temperature range of 308–1078 K. FTIR spectra (KBr pellets) were recorded on a Shimadzu 8201 PC spectrophotometer in the 400–4000 cm^{-1} region.

2.3. Acidity measurements

IR spectra of pyridine adsorbed on titanosilicates were recorded on a Shimadzu SSU 8000 DRIFT-IR spectrometer equipped with a liquid nitrogen-cooled MCT detector. Samples were activated at 698 K for 2 h under nitrogen flow, then cooled to 323 K, and pyridine (30 μL) was adsorbed. The sample temperature was raised to a desired value and held at that temperature for 30 min, after which the spectrum was recorded.

Temperature-programmed desorption (TPD) of ammonia was performed on a Micromeritics Autochem 2910 instrument. Titanosilicates (500 mg) were first activated at 773 K for 2 h in He flow (20 mL/min), then cooled to 353 K, after which 10% NH_3 in He was adsorbed for 30 min. The samples were flushed with He (30 mL/min) for 1 h at 373 K, and the desorption was monitored by raising the temperature from 373 to 723 K at a ramp rate of 10 K/min. In the case of SBA-15-*pr*-SO_3H (50 mg), the sample was first activated at 423 K for 1 h in He flow (5 mL/min), then cooled to 298 K, after which 10% NH_3 in He was adsorbed for 1 h. The sample was flushed with He (10 mL/min) for 30 min at 373 K, and the desorption of NH_3 was measured by raising the temperature from 373 to 923 K at a ramp rate of 10 K/min and holding it at 923 K for 20 min. Because sulfonic acid groups were thermally unstable beyond 475 K, only the desorption of NH_3 at 373–473 K was considered for the present work.

2.4. Ion-exchange capacity of SBA-15-pr-SO_3H

About 50 mg of SBA-15-*pr*-SO_3H was dispersed in 10 mL of 0.01 M NaCl solution and allowed to equilibrate for about 30 min. Then the solid was separated out, and the liquid portion was titrated with 0.01 M NaOH solution. The ion-exchange capacity of the catalyst was determined from the titration value [44].

In some studies, SBA-15-*pr*-SO_3H was initially adsorbed with different amounts (0.25–1.5 mmol) of styrene oxide or aniline. Ion-exchange capacities of these modified catalysts were determined in the same manner as described above. Thus, the influence of substrate adsorption on the ion exchange capacity of SBA-15-*pr*-SO_3H was determined.

2.5. Reaction procedure

2.5.1. Reaction of epoxides and amines: Synthesis of β-amino alcohols

In a typical reaction, known quantities of catalyst and epoxide and an equimolar quantity of amine were added to a double-necked round-bottomed flask (50 mL) placed in a temperature-controlled oil bath and fitted with a water-cooled condenser. The reaction was conducted at a specified temperature and for a specified period. The progress of the reaction was monitored by obtaining an aliquot of the sample, diluting it with a known quantity of dichloromethane, separating the catalyst by centrifugation, and subjecting the diluted liquid to gas chromatographic analysis (Varian 3400; CP-SIL8CB column; 30 m long and 0.53 mm i.d.). The products were identified by GC–MS (Varian CP-3800; 30 m long, 0.25 mm i.d., with a 0.25-μm-thick CP-Sil8CB capillary column). They were also isolated by column chromatography (eluent: petroleum ether–ethyl acetate mixture) and characterized by ^{1}H NMR studies. The characteristics of some isolated products are as follows:

2-Phenylamino-2-phenyl ethanol: GC–MS (*m*/*e*): 214.8, 213.8, and 182.0. ^{1}H NMR: 3.7 (1H, dd), 3.9 (1H, dd), 4.4 (1H, dd), 6.5 (2H, d), 6.7 (1H, t), 7.1 (2H, t), 7.3 (5H, m).

2-(4-Chlorophenylamino)-2-phenyl ethanol: GC–MS (*m*/*e*): 249.1, 248.2, and 246.3. ^{1}H NMR: 3.7 (1H, dd), 3.9 (1H, dd), 4.4 (1H, dd), 6.5 (2H, d), 7.05 (2H, d), 7.4 (5H, m).

2-(3-Methylphenylamino)-2-phenyl ethanol: GC–MS (*m*/*e*): 228.0, 227.4, 197.3, 196.4, and 118.1. ^{1}H NMR: 2.3 (3H, s), 3.7 (1H, dd), 3.9 (1H, dd), 4.5 (1H, dd), 6.5 (3H, m), 7.0 (1H, t), 7.3 (5H, m).

2-(2-Methylphenylamino)-2-phenyl ethanol: GC–MS (*m*/*e*): 228.0, 227.4, 197.3, 196.4, and 118.1. ^{1}H NMR: 2.3 (3H, s), 3.8 (1H, dd), 3.9 (1H, dd), 4.5 (1H, dd), 6.37 (1H, d), 6.63 (1H, t), 6.95(1H, t), 7.07 (1H, d), 7.35 (5H, m).

Kinetic studies were done by classic methods, taking different molar ratios of reactants and conducting the experiments at different temperatures.

2.5.2. Reaction of epoxides and alcohols: Synthesis of β-alkoxy alcohols

Equimolar amounts of styrene oxide and alcohol and known quantities of the catalyst were reacted in a 50-mL double-necked, round-bottomed flask placed in a temperature-controlled oil bath and fitted with a water-cooled condenser. The progress of the reaction and analysis of the products were determined as described in Section 2.5.1.

3. Results and discussion

3.1. Composition and structure-texture characterization of catalysts

3.1.1. SBA-15 functionalized with propylsulfonic acid

The elemental compositions of the functionalized-SBA-15 materials are given in Table 1. Propylsulfonic acid-functionalized SBA-15 was prepared by the postgrafting technique. In the first step, SBA-15-*pr*-SH was prepared by condensation of a preformed, vacuum-dried SBA-15 with MPTMS [37–39]. In the second step, this was oxidized with aqueous H_2O_2 to the sulfonic acid functionality (SBA-15-*pr*-SO_3H) [40–42]. MPTMS has three potential sites [–Si(OCH_3)$_3$] for binding with the silica surface. Although in principle, all three sites can react with surface silanol groups to form Si–O–Si bonds, it is also possible that only one or two of the alkoxy groups will react with surface silanol groups. Possibly, the groups grafted via mono and, to some extent, bidentate modes can leach out initially during reactions. In addition, two of the SH-propyltrimethoxysilane molecules also may react with each other, forming direct Si–O–Si bonds between the organic functional molecules. However, at the low concentrations of functional groups used in the present study, such disulfide (S–S) bond formation was not detected by spectral analysis.

The SBA-15 materials showed an XRD pattern (Fig. 1a) corresponding to a two-dimensional hexagonal *p6mm* symmetry [37–42]. Well-resolved (100), (110), and (200) reflections, consistent with a long-range mesopore ordering for SBA-15, appeared at 2θ values of 0.919, 1.570, and 1.809°, respectively. On organo-functionalization, these peaks shifted to higher 2θ values: 1.019, 1.755, and 2.035° for SBA-15-*pr*-SH and 1.034, 1.779, and 2.059° for SBA-15-*pr*-SO_3H (Fig. 1a). Shift in the peak positions to higher 2θ values also have been reported by other researchers when transition metal ions and metal complexes were introduced into mesoporous architectures [37–42]. The *d*-spacing (d_{100}) and unit cell parameters (Table 1) agree well with previously reported values [37–42].

Organic functionalization did not alter the long-range mesoporous arrangement (Fig. 2). In general, the catalysts exhibited type IV nitrogen adsorption/desorption isotherms with H1 hysteresis. On organic functionalization, a marked decrease in BET surface area (from 692 to 533 m^2/g) and total pore volume (from 1.13 to 0.83 cm^3/g) was detected (Table 1). The pore diameters were in the range of 6.2–6.5 nm, corresponding to mesopores [37–42]. The value of the C constant of the BET equation decreased from 1.05×10^2 (for SBA-15) to 0.78×10^2 for SBA-15-*pr*-SH and 0.83×10^2 for SBA-15-*pr*-SO_3H, due to the elimination of acidic surface OH on silylation. In such cases, the BET theory does not apply. However, the surface area determined by BJH using the cumulative area of the pores also showed a similar decrease as a consequence of organic functionalization (Table 1). Thus, this large decrease in surface area on functionalization with a few molecules of modifier (-*pr*-SH and -*pr*-SO_3H) is rather surprising. Apparently some reconstruction of the solid occurred that we were not able to detect.

SBA-15 shows characteristic IR peaks at around 1040–1260, 820, and 500 cm^{-1} due to Si–O–Si stretching vibrations and a broad, asymmetric feature at 2900–3800 cm^{-1} due to the O–H of silanols and water (Fig. 1b) [37–39]. Functionalization with -*pr*-SH showed additional features at 2928 and 2852 cm^{-1} due to C–H stretching vibrations and a weak peak at 2575 cm^{-1}, confirming the presence of SH functionality in the solid [37–39]. In the case of SBA-15-*pr*-SO_3H, the band at 2575 cm^{-1} was completely absent, indicating that the –SH groups originally present in SBA-15-*pr*-SH were all oxidized

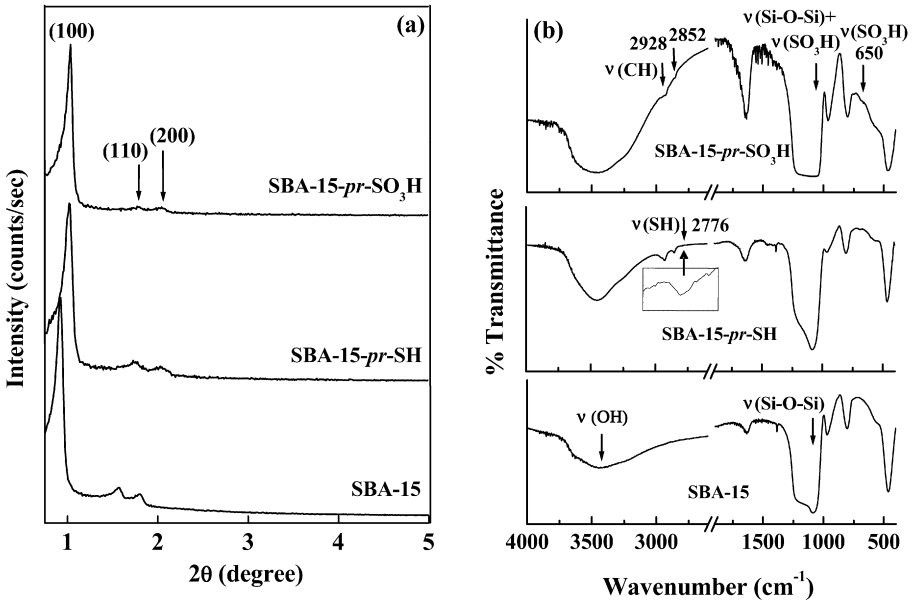

Fig. 1. (a) X-ray diffractograms and (b) FTIR spectra of "neat" and organo-functionalized SBA-15. Characteristic IR peaks are indicated by arrows.

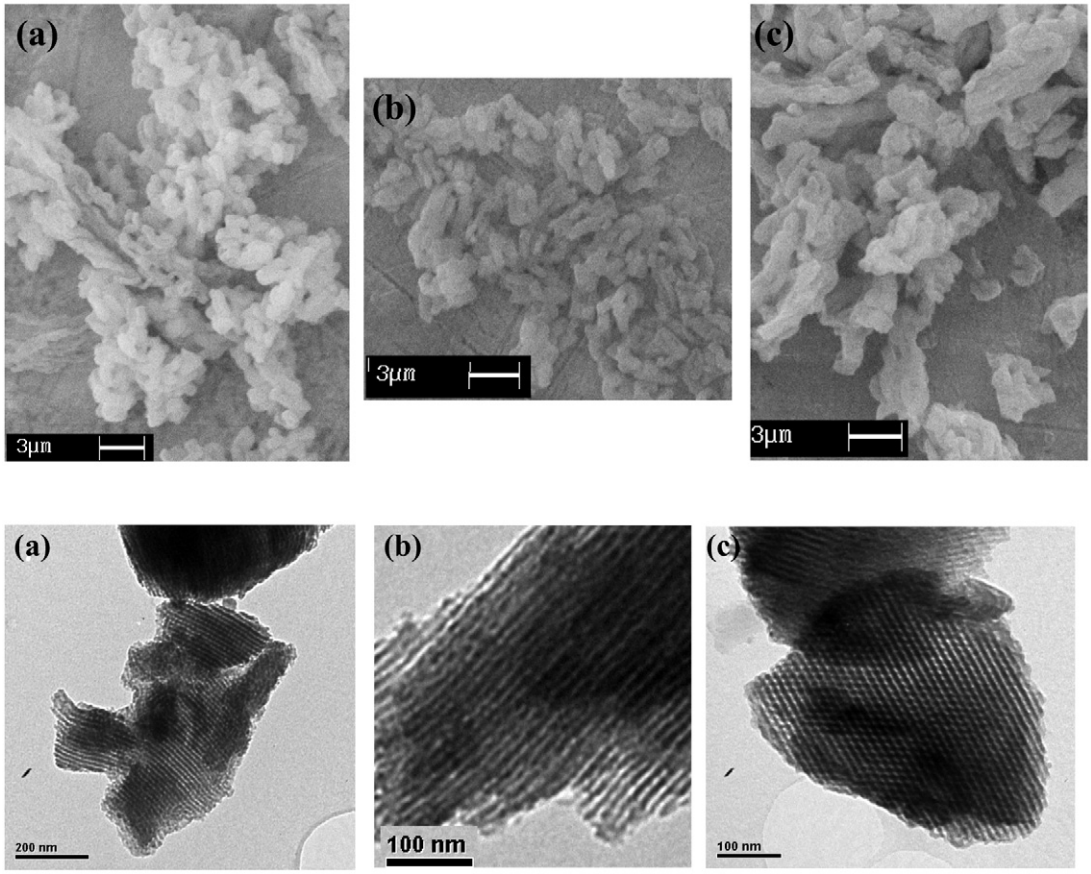

Fig. 2. Scanning electron micrographs (top) and transmission electron micrographs (bottom) of (a) SBA-15, (b) SBA-15-*pr*-SH and (c) SBA-15-*pr*-SO_3H.

to $-SO_3H$ groups. The sulfonic acid group showed bands at 650 and 1060 cm^{-1} in SBA-15-*pr*-SO_3H [40–42].

Thermogravimetric analysis of SBA-15 showed three stages of weight loss: stage I (313–475 K, exothermic), corresponding to the loss of physically held water; stage II (475–815 K, exothermic), corresponding to the loss of water within the micropore walls; and stage III (815–1273 K, endothermic), due to silanol condensation [26,45]. SBA-15-*pr*-SH and SBA-15-*pr*-SO_3H showed four stages of weight loss: stages I, IIA, IIB, and III. Stages IIA (475–661 K) and IIB (661–815 K) are due to

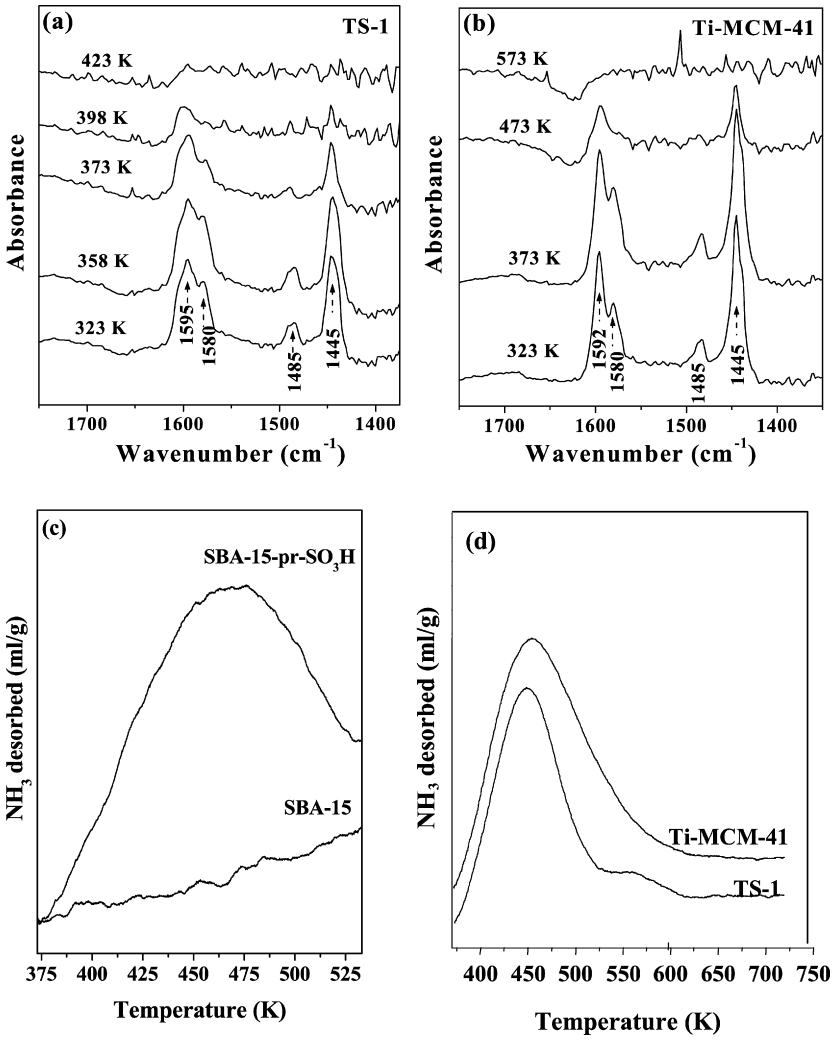

Fig. 3. DRIFT spectra of adsorbed pyridine on (a) TS-1 and (b) Ti-MCM-41. NH_3-TPD: (c) functionalized SBA-15 and (d) titanosilicate catalysts.

desorption of water from the micropore walls, as well as decomposition of the organic functional groups [26,45]. The amount of organic functional groups grafted was estimated from the weight losses; this value agreed well with that estimated from the elemental analyses data (Table 1).

3.1.2. Titanosilicates

The crystallinity and phase purity of TS-1 and Ti-MCM-41 samples were confirmed based on their XRD patterns [31]. FTIR and diffuse-reflectance UV–visible spectroscopy techniques confirmed the framework substitution of Ti in titanosilicates [28]. The textural properties of Ti-MCM-41 are as follows: $S_{BET} = 1055\ m^2/g$; pore volume $= 0.77\ cm^3$, and average pore diameter $= 29.4$ Å.

3.2. Acidic properties

3.2.1. DRIFT spectroscopy

The acidic properties of the samples were determined by DRIFT spectroscopy of adsorbed pyridine and NH_3-TPD measurements. The samples showed peaks at around 1595 and 1445 cm^{-1} due to H-bonded pyridine and at 1580 and 1485 cm^{-1} due to pyridine-coordinated to weak Lewis acid sites (Figs. 3a and 3b). Strong Lewis acid sites (peaks at 1623 and 1455 cm^{-1}) and Brönsted sites (peaks at 1639 and 1546 cm^{-1}) were absent. The IR bands were relatively more intense in Ti-MCM-41 than in TS-1, consistent with the easier accessibility of the Ti sites to pyridine in the former than in the latter. The IR peaks due to pyridine disappeared completely above 398 K on TS-1 and above 523 K on Ti-MCM-41, suggesting that the Lewis acid sites are stronger on Ti-MCM-41 than on TS-1. Easy accessibility of Ti sites in Ti-MCM-41 with an open tetrahedral $Ti(OH)(OSi)_3$ structure leads to a higher concentration of Ti-pyridine complexes compared with Ti in TS-1.

3.2.2. NH_3-TPD and ion-exchange capacity

The organic functional groups on SBA-15-*pr*-SO_3H are thermally unstable beyond 475 K (Section 3.1.1). Thus, acidity estimation from NH_3-TPD may not be an accurate method for sulfonic acid-functionalized SBA-15 samples. Neat SBA-15 did not desorb NH_3 in the temperature range 373–473 K (Fig. 3c). SBA-15-*pr*-SO_3H showed a desorption peak with a maximum at 470 K; 0.26 mmol/g of catalyst was desorbed.

Table 2
Aminolysis of epoxides over SBA-15-*pr*-SO_3H and Ti-MCM-41

Run No.	Epoxide	Amine	SBA-15-*pr*-SO_3H[a]				Ti-MCM-41[b]			
			Epoxide conversion (mol%)	Product selectivity (%)		TOF[c] (h^{-1})	Epoxide conversion (mol%)	Product selectivity (%)		TOF[c] (h^{-1})
				A	B			A	B	
1	Epichlorohydrin	Aniline	92.6	100	0	165	76.6	100	0	161
2	Epichlorohydrin	*m*-Toluidine	58.0	87.0	13.0	103	83.6	85.0	15.0	175
3	Epichlorohydrin	*n*-Butyl amine	87.5	87.0	13.0	156	80.8	98.0	2.0	170
4	Epichlorohydrin	Dibutyl amine	36.3	92.6	7.4	65	92.2	90.8	9.2	194
5	Propene oxide	Aniline	59.7	100	0	107	86.3	81.0	19.0	181
6	Styrene oxide	Aniline	38.1	89.8	10.2	68	80.5	93.8	6.2	169
6a			(54.2)[d]	(92.6)[d]	(7.4)[d]	(24)[d]				
6b			(4.6)[e]	(100)[e]	(0)[e]					
7	Styrene oxide	*p*-Chloroaniline	34.0	94.4	5.6	61	70.1	94.2	5.8	147
8	Styrene oxide	*p*-Anisidine	15.0	100	0	27	50.0	96.2	3.8	105
9	Styrene oxide	*m*-Toluidine	32.3	88.2	11.8	58	72.9	94.5	5.5	153
10	Styrene oxide	*o*-Toluidine	19.1	100	0	34	68.8	95.8	4.2	144
11	Styrene oxide	Cyclohexylamine	10.0	85.0	15.0	18	12.6	92.4	7.6	26
12	Styrene oxide	*n*-Butyl amine	7.2	100	0	13	3.6	100	0	7
13	Styrene oxide	Piperidine	89.1	99.4	0.6	159	54.4	95.1	4.9	114
14	Styrene oxide	Morpholine	44.6	94.8	5.2	80	51.3	93.7	6.3	108
15	Cyclohexene oxide	Aniline	23.8	100	0	43	32.7	100	0	68

[a] *Reaction conditions:* SBA-15-*pr*-SO_3H, 25 mg (-*pr*-SO_3H loading was 0.56 mmol/g); epoxide, 10 mmol; amine, 10 mmol; temperature, 298 K; reaction time, 4 h.
[b] *Reaction conditions:* Ti-MCM-41 (Si/Ti = 35), 50 mg; epoxide, 20 mmol; epoxide:amine (molar ratio), 1:1; temperature, 308 K, reaction time, 4 h.
[c] Turnover frequency (TOF) = moles of epoxide converted per mol of $–SO_3H$ or Ti in the catalyst per hour.
[d] Reaction conducted with 100 mg of the catalyst.
[e] Reaction conducted in the absence of a catalyst.

Based on the titrimetric method, we found that the ion-exchange capacity of this sample was 0.7 mEq/g catalyst, which is in good agreement with the expectation from thermal and elemental analyses of $–SO_3H$ groups. This suggests that in SBA-15-*pr*-SO_3H, almost all of the protons of sulfonic acid can be exchanged with sodium ions. Titrimetric studies also were conducted for thiol-functionalized SBA-15 (SBA-15-*pr*-SH) and "bare" SBA-15. The ion-exchange capacities of these materials were 0.2 and 0.04 mEq/g catalyst, respectively. Note that the ion-exchange capacity of SBA-15-*pr*-SH was much lower than the actual thiol content of the catalyst (Table 1); thus, only a fraction of the surface SH protons were replaced by Na^+. Because the thiol group is a weaker acid than the sulfonic acid, the dissociation of the S–H protons and consequent ion exchange with Na^+ are lower for SBA-15-*pr*-SH than for SBA-15-*pr*-SO_3H.

NH_3-TPD studies on titanosilicates revealed a desorption peak at 448 K (Fig. 3d). This desorption was more intense and asymmetric in Ti-MCM-41, indicating, in agreement with the DRIFT studies, the differences in the greater strength of the Lewis acid sites. This differences in accessibility and acid strength of Ti sites in TS-1 and Ti-MCM-41 influence their catalytic activity.

3.3. Catalytic activity

3.3.1. Aminolysis of epoxides

β-Amino alcohols were synthesized by the ring opening of epoxides with amines over SBA-15-*pr*-SO_3H, TS-1 and Ti-MCM-41 catalysts at ambient temperatures and under solvent-free conditions (Table 2). Both steric hindrance and nucleophilicity of the amine influenced the reactivity.

The reaction of styrene oxide with aniline yielded two types of regio-isomers: A and B (Scheme 1). Selectivity for the A-isomer was always higher (Table 2). The intrinsic catalytic activity (turnover frequency [TOF]) of SBA-15-*pr*-SO_3H was higher than all of the hitherto known catalysts for this reaction [8–16]. For example, for the reaction between styrene oxide and aniline, TOF values over sulfamic acid, amberlyst-15, $Sc(OTf)_3$, and NaY catalysts were 32, 2, 7, and 0.8 h^{-1}, respectively [8–16]. The corresponding value for SBA-15-*pr*-SO_3H was found to be 68 h^{-1} (Table 2).

Very high conversion (92.6 mol%) and selectivity of product-A (100 mol%) were obtained when epichlorohydrin instead of styrene oxide was reacted with aniline (Table 2, run 1). Despite the fact that epichlorohydrin has many reactive positions and can in principle lead to some other products, we did not observe (by gas chromatography) products other than the amino alcohols A and B. Moreover, the conversions estimated based on the disappearance of either of the two reactants (epoxide/amine) were about the same. The reactivity (% conversion) decreased in the following order: epichlorohydrin > propene oxide > styrene oxide > cyclohexene oxide. Cyclohexene oxide is a symmetrical epoxide. Reaction with aniline yielded *cis*- and *trans*-diastereomeric products (Scheme 1). Only the *trans*-diastereo isomer was formed (product characterization by ^1H NMR study) with 100% selectivity over these catalysts (Table 2, run 15).

Table 3
Influence of Ti structure: reaction of styrene with aniline over different catalysts[a]

Catalyst	Styrene oxide conversion (%)	Product selectivity (%)		TOF (h^{-1})[b]
		A	B	
Nil	6.6	89.7	10.3	–
TS-1	11.5	90.8	9.2	24
Ti-MCM-41	80.5	93.8	6.2	169
Ti-MCM-41, 1st recycle	77.4	95.1	4.9	162
Ti-MCM-41, 2nd recycle	77.0	94.2	5.8	162
TiO_2 (2 mg)	9.1	86.0	14.0	18
TiO_2 (50 mg)	48.0	86.3	13.7	4

[a] *Reaction conditions:* catalyst (TS-1/Ti-MCM-41 (Si/Ti = 35)), 50 mg; styrene oxide, 20 mmol; styrene oxide:aniline (molar ratio), 1:1; reaction time, 4 h; reaction temperature, 308 K.

[b] Turnover frequency (TOF) = moles of epoxide converted per mol of Ti in the catalyst per hour.

A range of β-amino alcohols was produced with high regioselectivity from styrene oxide and different amines. The reactivity (epoxide conversion and TOF) depended on the nature and type of the amine molecule, however. The product yield was low when cyclohexyl amine instead of aniline was used. High conversions were obtained with aliphatic amines like *n*-butyl amine (Table 2, run 3). With the secondary amine piperidine, conversion of 89.1 mol% and product isomer-A selectivity of 99.4 mol% were obtained (Table 2, run 13). However, with morpholine, which contains an additional oxygen atom in the hexa-cyclic saturated ring, the conversion was only 44.6 mol% (run 14).

We also conducted the reaction of styrene oxide with aniline at 298 K in the presence of thiol-functionalized SBA (SBA-15-*pr*-SH) and "bare" SBA-15. Conversions of styrene oxide in those experiments were only 29 and 24.6 mol%, in contrast to 38.1 mol% in the presence of SBA-15-*pr*-SO_3H (Table 2, run 6). These variations in catalytic activity follow changes in the ion-exchange capacities/acid strengths of these SBA-15 materials. Whereas isomers A and B (with product selectivity of 89.8 and 10.2 mol%, respectively) formed over SBA-15-*pr*-SO_3H, only the isomer-B formed over SBA-15-*pr*-SH and SBA-15.

Over Ti-MCM-41 catalysts, a styrene oxide conversion of 80 mol% and isomer-A selectivity of 93.8 mol% were obtained at 308 K (Table 2, run 3) [19]. At similar reaction conditions, TS-1 showed only 11.5 mol% conversion and 90.8 mol% of A-isomer product selectivity (Table 2, run 2). Due to diffusion limitations, the reaction over TS-1 occurs mainly at the outer surface of particles [19].

We also carried out experiments with anatase-TiO_2. The Ti content in the sample was kept the same as that used in the experiments with Ti-MCM-41. The conversion was much lower over anatase-TiO_2 (9.1 mol%) than on Ti-MCM-41 (Table 3; compare runs 6 and 3). These findings indicate that dispersion and surface accessibility of the Ti^{4+} ions are important in determining the catalytic activity of titanosilicate materials.

To check the recyclability of the catalyst, the recovered catalyst was washed first with dichloromethane and then with methanol, then dried at 373 K for 2 h before reuse (Table 3, runs 4 and 5). On Ti-MCM-41, aminolysis with aromatic amines yielded higher conversion than aminolysis with aliphatic *n*-butyl amine. The product yields were also significantly higher on terminal epoxides than on symmetrical cycloalkene oxides. In general, the catalytic activity (TOF) of Ti-MCM-41 catalysts was higher than that of SBA-15-*pr*-SO_3H.

The use of solvents suppressed catalytic activity (Table 4). Solvent molecules compete with the substrate molecules for adsorption on the surface (refer to the discussion on adsorption studies presented later). The conversion was higher in nonpolar and weakly polar solvents (e.g., dichloromethane, toluene) than in polar solvents (e.g., acetonitrile, ethyl acetate) (Table 4).

Temperature had a notable effect on catalytic activity but only a marginal effect on selectivity (Table 5). Fig. 4 shows the influence of reaction time and temperature on styrene oxide conversion and product selectivity over Ti-MCM-41. The conversion increased with reaction time, but the product selectivity was unaffected. At near-ambient conditions, complete conversion of styrene oxide and very high selectivity of the A-type regioisomer (97.6 mol%) were obtained (Fig. 4i).

3.3.2. Alcoholysis of epoxides

SBA-15-*pr*-SO_3H demonstrated catalytic activity for the reaction of styrene oxide with different alcohols at ambient temperature and solvent-free conditions (Table 6). Selectivity of product A (Scheme 1) was 100%. The intrinsic catalytic activity of SBA-15-*pr*-SO_3H was significantly higher compared with the hitherto known catalysts [17]. Both products A and B were detected over Ti-MCM-41, with A being the major one.

3.4. Kinetic studies

The kinetic rate constants and apparent activation energies for the aminolysis of styrene oxide with aniline over SBA-15-*pr*-SO_3H and Ti-MCM-41 catalysts were determined using different molar ratios of the reactants and at different temperatures. The reaction was first order with respect to both styrene oxide and aniline. The apparent activation energies (E_a) were calculated using the Arrhenius equation, $k = A\exp(-E_a/RT)$. These values for both solid acid catalysts are listed in Table 7. The rate constants were higher and the activation energy was lower over Ti-MCM-41 than over SBA-15-*pr*-SO_3H. Brönsted-acidic SBA-15-*pr*-SO_3H possibly protonates the amines instead of activating the epoxide molecules. Thus, the Lewis acid (Ti-MCM-41) is likely more active.

3.5. Mechanistic considerations

Aminolysis of epoxides is a bimolecular reaction. An additional factor, not present in homogeneous catalysis, can influence the rate and mechanism of the reaction in catalysis over solid catalysts: the competitive access of the epoxide and amine molecules to the acidic, active sites on the surface. The different basicities of the amine and epoxide can influence their relative surface coverages and, consequently, the reaction rates.

Adsorption of one substrate (epoxide or amine), as well as competitive adsorption of both, were investigated. In the ad-

Table 4
Influence of solvent on the adsorption characteristics and reaction of styrene oxide with aniline over SBA-15-*pr*-SO_3H and Ti-MCM-41[a]

Solvent (dielectric constant)	SBA-15-*pr*-SO_3H						Ti-MCM-41			
	One substrate adsorption (mmol/g catalyst)[b]		Epoxide conversion (mol%)	Product selectivity (mol%)		TOF (h^{-1})[c]	Epoxide conversion (mol%)	Product selectivity (mol%)		TOF (h^{-1})[c]
	Styrene oxide	Aniline		A	B			A	B	
No solvent	0.20	0.21	38.1	89.8	10.2	68	99.5	97.6	2.4	52
Dichloromethane (9.1)	0.20	0.21	33.7	62.0	38.0	30	77.6	99.2	0.8	8
Carbon tetrachloride (2.2)							71.2	98.8	1.2	7
Toluene (2.4)	0.17	0.20	26.4	100	0	24	81.0	98.8	1.2	9
Acetonitrile (37.5)	0.06	0.13	4.1	100	0	4	25.0	98.6	1.4	3
Ethyl acetate (6.0)	0.04	0.11	3.9	100	0	3	27.7	97.6	2.4	3

[a] *Reaction conditions:* SBA-15-*pr*-SO_3H (-*pr*-SO_3H loading is 0.56 mmol/g); catalyst, 25 mg; styrene oxide, 5 mmol (with solvent) or 10 mmol (without solvent); reaction temperature, 298 K. Ti-MCM-41 (Si/Ti = 35); catalyst, 50 mg; styrene oxide, 1 mmol (with solvent) or 5 mmol (without solvent); reaction temperature, 303 K. Solvent, 0 or 5 mL; styrene oxide:aniline (molar ratio), 1:1; reaction time, 4 h.

[b] Activated (393 K for 4 h) SBA-15-*pr*-SO_3H (50 mg) was dispersed, for 1 h, in 0.5 mmol of styrene oxide or aniline substrate dissolved in 5 mL of solvent. The solid catalyst was, then, separated and the concentration of the substrate in the liquid portion was determined by gas chromatography. The amount adsorbed on the catalyst surface was determined by difference.

[c] Turnover frequency (TOF) = moles of epoxide converted per mol of –SO_3H or Ti in the catalyst per hour.

Table 5
Influence of temperature on the reaction of styrene oxide with aniline over SBA-15-*pr*-SO_3H and Ti-MCM-41[a]

SBA-15-*pr*-SO_3H[a]					Ti-MCM-41[b]				
Reaction temperature (K)	Epoxide conversion (%)	Product selectivity (%)		TOF (h^{-1})[c]	Reaction temperature (K)	Epoxide conversion (%)	Product selectivity (%)		TOF (h^{-1})[c]
		A	B				A	B	
298	38.1	89.8	10.2	68	272	20.2	96.0	4.0	85
308	68.5	86.3	13.7	122	293	31.4	96.2	3.8	132
323	88.7	87.1	12.9	158	303	50.9	95.3	4.7	214
343[d]	91.3 (9.0)	83.6 (83.9)	16.4 (16.1)	163	308	77.1	94.4	5.6	324
					323	88.0	93.5	6.5	370
					343	97.6	92.3	7.7	410

[a] *Reaction conditions:* catalyst, 25 mg; styrene oxide, 10 mmol; styrene oxide:aniline (molar ratio), 1:1; reaction time, 4 h.

[b] *Reaction conditions:* catalyst, 50 mg; styrene oxide, 20 mmol; styrene oxide:aniline (molar ratio), 1:1; reaction time, 2 h.

[c] Turnover frequency (TOF) = moles of epoxide converted per mol of –SO_3H or Ti in the catalyst per hour.

[d] Values in parentheses are those with no catalyst.

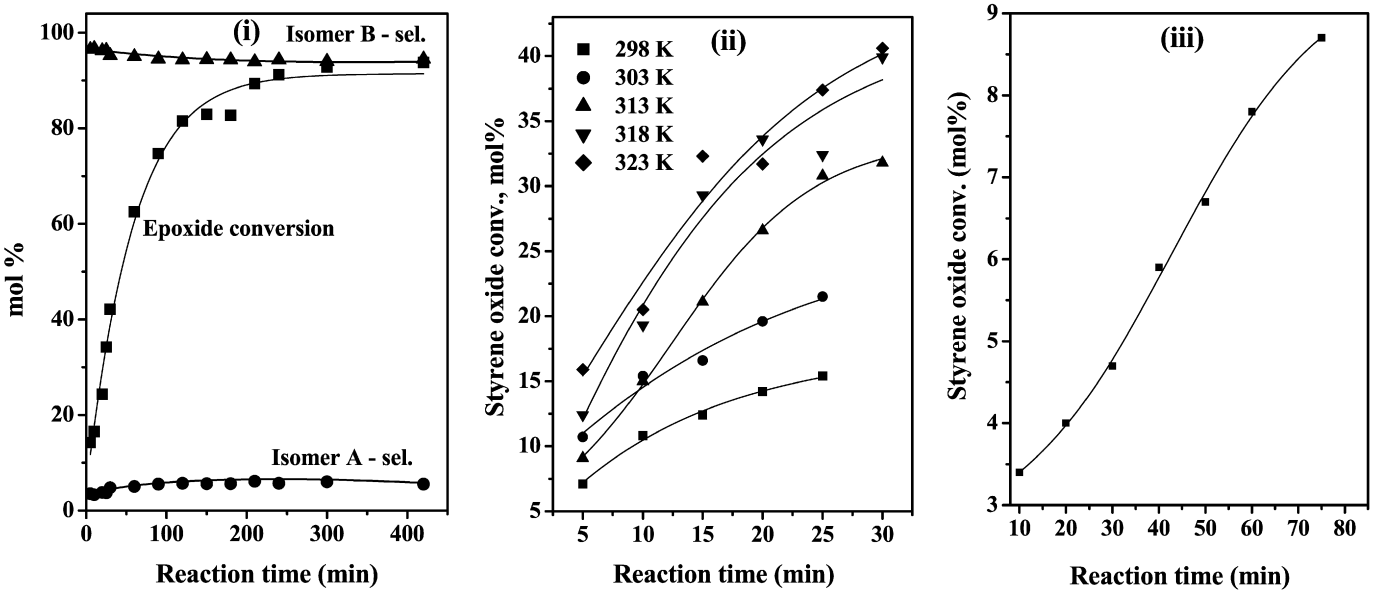

Fig. 4. Aminolysis of styrene oxide. (i) Influence of reaction time: reaction conditions—styrene oxide, 40 mmol; aniline, 40 mmol; Ti-MCM-41, 100 mg; temperature, 308 K. (ii) Influence of temperature: reaction conditions—styrene oxide, 20 mmol; aniline, 20 mmol; Ti-MCM-41, 50 mg. (iii) Reaction over SBA-15-*pr*-SO_3H. Influence of reaction time: reaction conditions—styrene oxide, 20 mmol; aniline, 20 mmol; SBA-15-*pr*-SO_3H, 50 mg.

Table 6
Alcoholysis of styrene oxide over SBA-15-*pr*-SO_3H and Ti-MCM-41[a]

Run No.	Alcohol	SBA-15-*pr*-SO_3H			Ti-MCM-41			
		Styrene oxide conversion (mol%)	Selectivity of product A	TOF (h^{-1})[b]	Styrene oxide conversion (mol%)	Product selectivity (mol%)		TOF (h^{-1})[b]
						A	B	
1	Methanol	25.6	100	23	27.8	88.0	12.0	29
2	Ethanol	16.8	100	15	15.2	87.3	12.7	16
3	Propanol	10.4	100	9	12.4	92.8	7.2	13
4	*n*-Butanol	9.2	100	8	11.1	92.9	7.1	11
5	Benzyl alcohol	6.2	100	5				
6	Cyclohexanol	7.2	100	6	8.1	78.9	21.1	8

[a] *Reaction conditions:* SBA-15-*pr*-SO_3H: catalyst, 25 mg; styrene oxide and alcohol, 5 mmol each; temperature, 298 K; reaction time, 4 h. Ti-MCM-41: catalyst, 50 mg; styrene oxide, 10 mmol; alcohol, 20 mmol; temperature, 333 K; reaction time, 4 h.
[b] Turnover frequency (TOF) = moles of styrene oxide converted per mol of $–SO_3H$ or Ti in the catalyst per hour.

Table 7
Kinetic data for aminolysis of styrene oxide with aniline over SBA-15-*pr*-SO_3H and Ti-MCM-41 catalysts[a]

Catalyst	Reaction temperature (K)	Rate constant ($L\ mol^{-1}\ s^{-1}$)	Activation energy (E_a) ($kJ\ mol^{-1}$)
SBA-15-*pr*-SO_3H	298	7.96×10^{-4}	59
	308	2.70×10^{-3}	
	313	2.75×10^{-3}	
	318	3.58×10^{-3}	
Ti-MCM-41	313	7.31×10^{-3}	37
	318	9.15×10^{-3}	
	323	11.31×10^{-3}	

[a] Reactions were conducted taking 1:1 molar ratio of styrene oxide to aniline. Amount of the catalyst: 25 mg (SBA-15-*pr*-SO_3H) or 50 mg (Ti-MCM-41).

sorption studies of one substrate, a known quantity of SBA-15-*pr*-SO_3H (50 mg) was initially activated at 393 K for 4 h and then dispersed at 298 K in a known concentration of the substrate (0.5 mmol) dissolved in a solvent (5 mL). After an hour, the concentration of the substrate in the liquid portion was estimated by gas chromatography, and the amount adsorbed was determined. When dichloromethane was used as a solvent, the amount of styrene oxide and aniline adsorbed on the catalyst surface were found to be 0.20 and 0.21 mmol/g catalyst, respectively (Table 4). Similar values were obtained when toluene was used as a solvent (Table 4). However, in the polar, aprotic acetonitrile, the amounts of epoxide as well as the amine adsorbed on the catalyst were considerably lower (0.06 and 0.13 mmol/g catalyst, respectively). Polar solvents compete with the substrate molecules for adsorption (on sulfonic acid groups) and thereby lower catalytic activity. Note that there exists an inverse correlation between the dielectric constant of the solvent and catalytic activity over Ti-MCM-41 (Table 4). In further studies, dichloromethane was selected as the solvent of choice, because it did not compete appreciably with the substrate molecules for adsorption on the catalyst surface (Table 4).

The influence of substrate adsorption on proton-exchange capacity of the catalyst was investigated by the titrimetric method (Section 2.4). When different amounts (0.25–1.5 mmol) of styrene oxide or aniline were adsorbed on the sulfonic acid-functionalized SBA-15, the ion-exchange capacity of the catalyst decreased from 0.73 mEq/g for SBA-15-*pr*-SO_3H to about 0.3 mEq/g for the epoxide- or amine-adsorbed catalyst (Fig. 5). Both the epoxide and aniline adsorb on the sulfonic acid functionality.

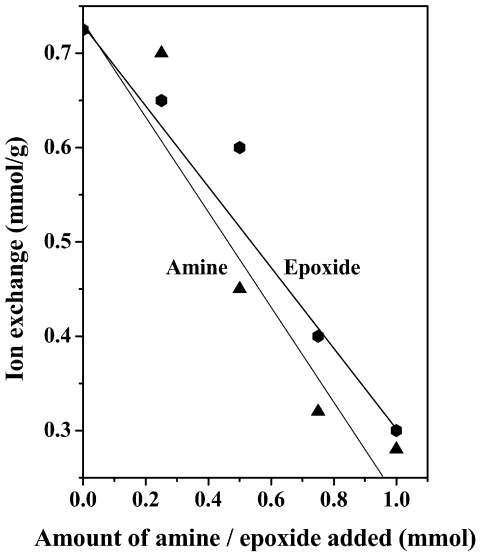

Fig. 5. Change in ion exchange capacity with the amount of preadsorbed epoxide or amine on SBA-15-*pr*-SO_3H.

In some experiments, aniline was preadsorbed on SBA-15-*pr*-SO_3H. Styrene oxide was then adsorbed. The catalytic activities of these aniline-preadsorbed catalysts were also determined simultaneously. Epoxide adsorption and catalytic activity decreased with increasing amounts of preadsorbed amine. Epoxide adsorption on the acid site was apparently essential for the reaction (Fig. 6a). In another set of experiments, different amounts of styrene oxide were initially added onto the SBA-15-*pr*-SO_3H surface. Thereafter, the amine adsorption capacity and catalytic activity of those modified catalysts were determined. The amount of aniline adsorption and catalytic activity increased with increasing amount of epoxide added (Fig. 6b). Aniline was consumed due to reaction with the epoxide already activated on the acidic site, yielding the product β-amino alcohol. There is a correlation between styrene oxide conversion and the amount of epoxide preadsorbed (Fig. 6c). The amounts

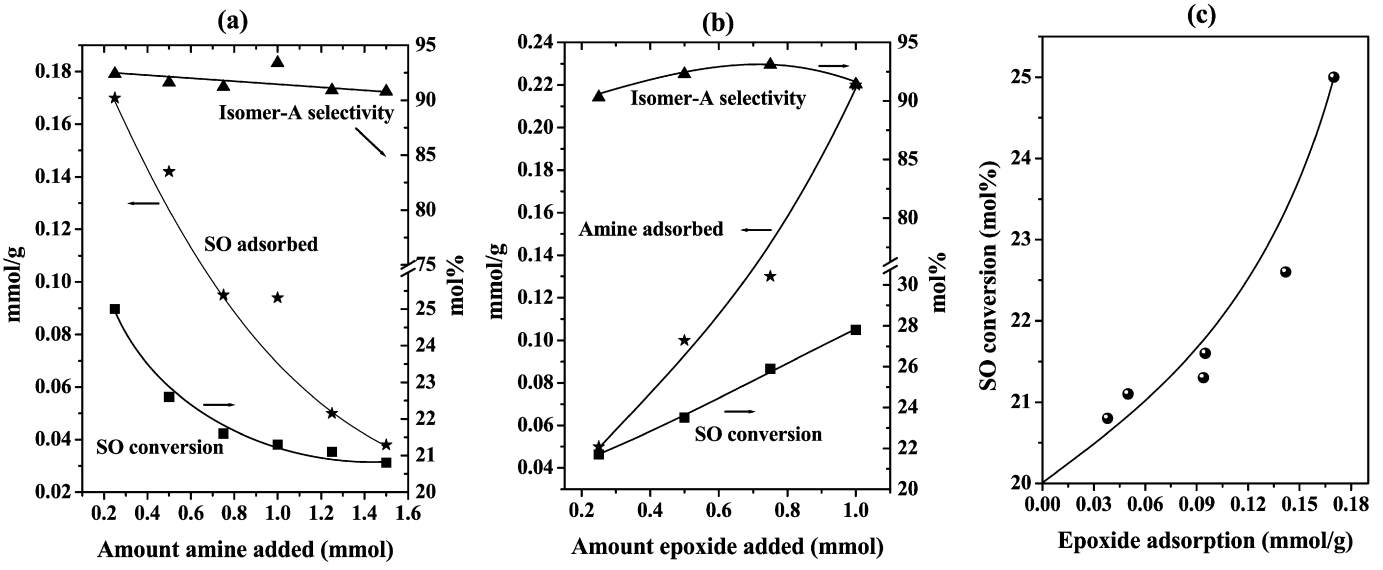

Fig. 6. SBA-15-*pr*-SO_3H. (a) Variation in styrene oxide adsorption and conversion with preadsorbed aniline. (b) Variation in aniline adsorption and styrene oxide conversion with preadsorbed styrene oxide. (c) Influence of preadsorbed amine on epoxide adsorption and catalytic activity in the reaction of styrene oxide (SO) with aniline.

Table 8
Epoxide and amine adsorptions on SBA-15-*pr*-SO_3H and Ti-MCM-41 catalysts[a]

Material	Amount of epoxide adsorbed (mmol/g)			Amount of amine adsorbed (mmol/g)		
	Epichloro-hydrin	Styrene oxide	Cyclo-hexene oxide	Piperidine	Aniline	4-Cl-aniline
SBA-15	0.09	0.04	0.17	0.02	0.01	0.09
SBA-15-*pr*-SO_3H	0.17	0.20	0.34	0.03	0.21	0.23
Ti-MCM-41	0.42	1.25	0.43	0.77	0.55	1.41

[a] 50 mg of activated SBA-15 material was dispersed, for 1 h, in 0.5 mmol of styrene oxide or aniline substrate dissolved in 5 mL of solvent. The solid was, then, separated and the concentration of the substrate in the liquid portion was determined by gas chromatography. The amount adsorbed on the catalyst surface was determined by difference. 100 mg of Ti-MCM-41 was dispersed in 1 mmol of styrene oxide or aniline dissolved in 10 mL of CH_2Cl_2.

of different epoxides or amines adsorbed per gram of SBA-15-*pr*-SO_3H (in one-substrate adsorption experiments) are given in Table 8. Adsorptions were also done on "bare" SBA-15. The amount of substrate adsorbed on the catalyst surface varied with the nature of the substrate molecule. Diffusion constraints were not expected over these mesoporous catalysts. Both epoxides and amines adsorbed even on "bare" SBA-15, the former more than the latter (Table 8). Functionalization of SBA-15 surface with propylsulfonic acid moieties enhanced the adsorption of epoxide as well as amine substrates, the latter more than the former (Table 8). The amount of substrate adsorbed increased with its increasing concentration in the solution; however, it was always lower than the molar equivalent of propylsulfonic acid moieties present on the catalyst surface. Surprisingly, the amount of epoxide or amine adsorbed was significantly greater on the weakly Lewis-acidic Ti-MCM-41 than on SBA-15-*pr*-SO_3H (Table 8). The larger concentration of acidic, surface Ti atoms (compared with the number of grafted –SO_3H groups), rather than the strength of acidity, is probably responsible for the greater adsorption capacity as well as catalytic activity of T-MCM-41.

Because adsorption is an essential prerequisite in many of the liquid-phase bimolecular reactions between epoxides and amines [46], we also conducted competitive adsorption experiments wherein the sulfonic acid-functionalized SBA-15 (50 mg) was suspended in equimolar (0.5 mmol) amounts of epoxide (cyclohexene oxide, epichlorohydrin, or styrene oxide) and amine (aniline or *o*-toluidine) dissolved in 5 mL of dichloromethane. The adsorption of both the epoxide and amine were estimated; Table 9 compares the relative adsorption of the various epoxides and amines and also gives the corresponding TOFs. The importance of carrying out competitive adsorption of the reactants (in addition to their independent adsorption data) can be demonstrated by comparing the data in Tables 8 and 9. In independent adsorption experiments, the amount of epoxides adsorbed on SBA-15-*pr*-SO_3H varied as epichlorohydrin (0.17) < styrene oxide (0.20) < cyclohexene oxide (0.34) (Table 8). However, in the presence of an amine (aniline), a reverse variation was observed: epichlorohydrin > styrene oxide > cyclohexene oxide (relative adsorption ratios of 1.8, 1.1, and 0.8, respectively) (Table 9). The corresponding relative rates (TOFs of 165, 68, and 43 h^{-1}) correlate better with data from the competitive adsorption experiments and illustrate the perils involved in drawing conclusions from adsorption of individual reactants without taking into account the competition from the others or the solvent. The conversion vs time plots for

Table 9
Competitive adsorption of epoxide and amine over SBA-15-*pr*-SO_3H[a]

Adsorbate substrates	Amount adsorbed (mmol/g catalyst)		Relative adsorption ratio: epoxide/amine	TOF (h^{-1})[b]
	Epoxide	Amine		
Epichlorohydrin + aniline	0.10	0.06	1.8	165
Styrene oxide + aniline	0.08	0.07	1.1	68
Cyclohexene oxide + aniline	0.10	0.13	0.8	43
Styrene oxide + *o*-toluidine	0.03	0.04	0.8	34

[a] 50 mg of sulfonic acid functionalized SBA-15 was suspended for 1 h in equimolar amounts (0.5 mmol) of epoxide and amine dissolved in 5 mL of dichloromethane. The catalyst was, then, separated and the concentration of the substrate in the liquid portion was determined by gas chromatography. The amount adsorbed on the catalyst surface was determined by difference.

[b] Turnover frequency (TOF) = moles of epoxide converted per mol of –SO_3H in the catalyst per hour.

both Ti-MCM-41 and SBA-15-*pr*-SO_3H were of sigmoid shape (Fig. 4), further confirming that the mechanism involves a competition between reactants for adsorption.

Fig. 7 further illustrates the competition between the epoxide (styrene oxide) and the amine or alcohol for the active site. The rate of the reaction decreased when the basicity of the amine or alcohol increased. These findings from the reaction of epoxides with amines are similar to our earlier results [32,33] in the reaction of epoxides with carbon dioxide to yield cyclic carbonates over amine-functionalized Ti-SBA-15. We had concluded that whereas CO_2 molecules are activated at basic amine sites, Lewis-acidic Ti^{4+} ions are the sites for adsorption and activation of the epoxide molecules [32,33]. The decreased styrene oxide conversion observed in high-dielectric constant solvents (Table 4) also supports the above picture. Highly polar solvents compete with the epoxide for adsorption on the acidic site. Thus, it is not surprising that the highest conversions were observed in the absence of any solvent (Table 4, row 1). As shown in Scheme 1, two regioisomers are theoretically possible. In almost all of our studies (Tables 2–6), the A isomer predominated. Substituent groups on the epoxide (like R in Scheme 1) influenced the orientation of the incoming moiety (R′NH and R′OH) by steric as well as electronic effects [46]; bulky R groups favored the B isomer. Under basic or neutral conditions, when a S_N2 attack of the reagent molecule (like $R'NH_2$ or R′OH) on the epoxide ring carbon atom led to products, the B isomer was dominant. Under acidic conditions, on the other hand, electronic effects (inductive and conjugative) determine the orientation [46]. These electronic effects can stabilize a positive charge on the carbon atom (of the epoxide ring) adjacent to R. This is facilitated if the reaction occurs by a S_N1 mechanism in which the transition state for the rate-determining step carries a partial positive charge on the carbon atom adjacent to R. Protonation of the epoxide oxygen (by the –SO_3H group over SBA-15-*pr*-SO_3H) or its coordination to Ti^{4+} (in Ti-MCM-41) apparently favors the S_N1 mechanism on both of these acidic catalysts and the consequent predominance of the A isomer. This picture is supported by our results over SBA-15-*pr*-SH and SBA-15, mentioned earlier, wherein the B isomer predominated over the A isomer. Propylthiol and silanol are weakly acidic and near-neutral functional groups, respectively, compared with propylsulfonic acid (refer to the ion-exchange capacities in Section 3.2.2); thus, the significant formation of the B isomer over SBA-15-*pr*-SH and bare SBA-15 is understandable.

4. Conclusion

Here the aminolysis of epoxides over Brönsted-acidic SBA-15 functionalized with propylsulfonic acid and Lewis-acidic Ti-MCM-41 is reported for the first time. These mesoporous, solid acid catalysts are highly active and selective at ambient temperatures and solvent-free conditions. A range of β-amino alcohols were synthesized with high regioselectivity and stereoselectivity by reacting symmetric or unsymmetric epoxides

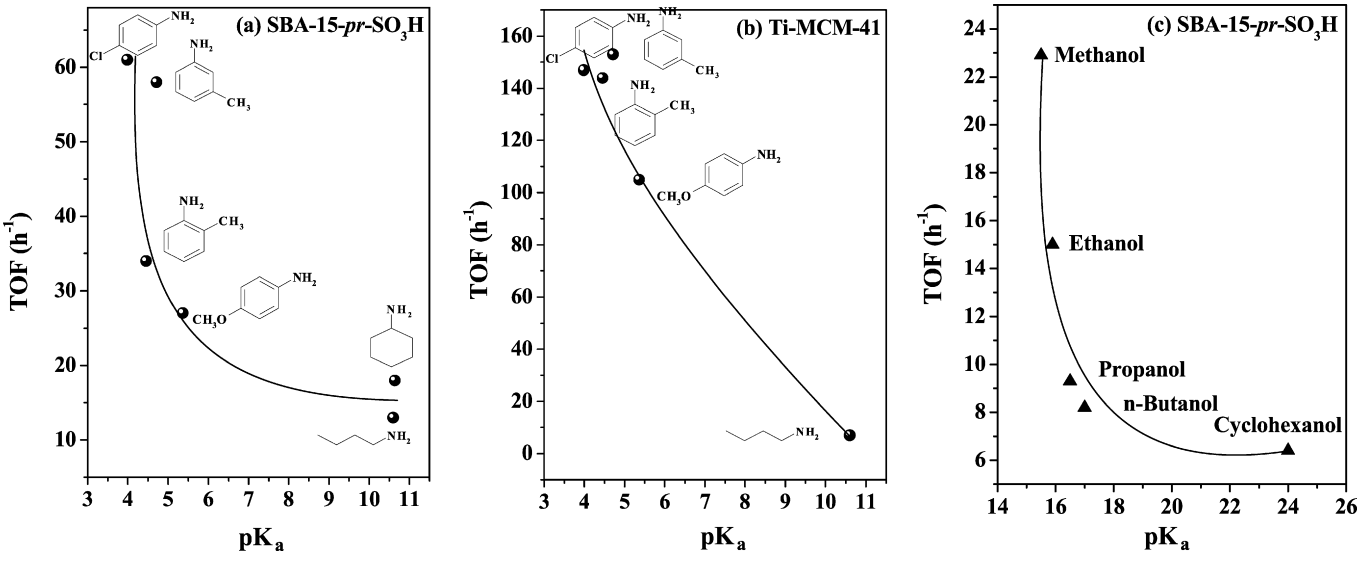

Fig. 7. Correlation between catalytic activity (turnover frequency; TOF) and pK_a of amine in aminolysis of styrene oxide over (a) SBA-15-*pr*-SO_3H and (b) Ti-MCM-41. (c) Correlation between TOF and pK_a of alcohols in alcoholysis of styrene oxide over SBA-15-*pr*-SO_3H.

with aromatic and aliphatic amines. Both of these catalysts exhibited significantly higher catalytic activity than the hitherto known acid catalysts for these reactions. Ti-MCM-41 was the more reactive of the two. Both epoxide and amine competed for adsorption on surface acid sites. Polar solvent molecules, when present, also competed for adsorption with the reactant molecules.

Acknowledgments

L.S. and J.K.S. acknowledge the Council of Scientific and Industrial Research (CSIR), New Delhi for a fellowship award.

References

[1] O. Mitsunobu, in: B.M. Trost, I. Fleming (Eds.), Comprehensive Organic Synthesis, vol. 6, Pergamon Press, New York, 1991, p. 88.
[2] E.J. Corey, F.-Y. Zhang, Angew. Chem. Int. Ed. Engl. 38 (1999) 1931.
[3] D.J. Ager, I. Prakash, D.R. Schaad, Chem. Rev. 96 (1996) 835.
[4] P. O'Brien, Angew. Chem. Int. Ed. Engl. 38 (1999) 326.
[5] G. Li, H.-T. Chang, K.B. Sharpless, Angew. Chem. Int. Ed. Engl. 35 (1996) 451.
[6] R.M. Hanson, Chem. Rev. 91 (1991) 437.
[7] P.A. Crooks, R. Szyudler, Chem. Ind. (London) (1973) 1111.
[8] A. Kamal, B. Rajendra Prasad, A. Malla Reddy, M. Naseer, A. Khan, Catal. Commun. 8 (2007) 1876.
[9] M. Vijender, P. Kishore, P. Narender, B. Satyanarayana, J. Mol. Catal. A Chem. 266 (2007) 290.
[10] A.T. Placzek, J.L. Donelson, R. Trivedi, R.A. Gibbs, S.K. De, Tetrahedron Lett. 46 (2005) 9029.
[11] J. Iqbal, A. Pandey, Tetrahedron Lett. 31 (1990) 575.
[12] R.I. Kureshy, S. Singh, N.H. Khan, S.H.R. Abdi, E. Suresh, R.V. Jasra, J. Mol. Catal. A Chem. 264 (2007) 162.
[13] F. Carrée, R. Gil, J. Collin, Org. Lett. 7 (2005) 1023.
[14] J.S. Yadav, B.V.S. Reddy, A.K. Basak, A.V. Narasaiah, Tetrahedron Lett. 44 (2003) 1047.
[15] P.-Q. Zhao, L.-W. Xu, C.G. Xia, Synlett (2004) 846 and 1122.
[16] N. Azizi, M.R. Saidi, Org. Lett. 7 (2005) 3649.
[17] R. Garcia, M. Martinez, J. Aracil, Chem. Eng. Technol. 22 (1999) 12.
[18] M.W.C. Robinson, R. Buckle, I. Mabbett, G.M. Grant, A.E. Graham, Tetrahedron Lett. 48 (2007) 4723.
[19] J.K. Satyarthi, L. Saikia, D. Srinivas, P. Ratnasamy, Appl. Catal. A Gen. 330 (2007) 145.
[20] J.A. Melero, R. van Grieken, G. Morales, Chem. Rev. 106 (2006) 3790.
[21] A. Vinu, K.Z. Hossain, K. Agira, Nanosci. Nanotechnol. 5 (2005) 347.
[22] I.K. Mbraka, D.R. Radu, V.S.Y. Lin, B.H. Shanks, J. Catal. 219 (2003) 329.
[23] W.D. Bossaert, D.E. De Vos, W.M. Van Rhijin, J. Bullen, P.J. Grobet, P.A. Jacobs, J. Catal. 182 (1999) 156.
[24] I. Diaz, C. Márquez-Alvarez, F. Mohino, J. Pérez-Pariente, E. Saste, Microporous Mesoporous Mater. 44–45 (2001) 295.
[25] B.C. Wilson, C.W. Jones, Macromolecules 37 (2004) 9709.
[26] L. Saikia, D. Srinivas, P. Ratnasamy, Appl. Catal. A Gen. 309 (2006) 144.
[27] L. Saikia, D. Srinivas, P. Ratnasamy, Microporous Mesoporous Mater. 104 (2007) 225.
[28] P. Ratnasamy, D. Srinivas, H. Knözinger, Adv. Catal. 48 (2004) 1.
[29] B. Notari, Adv. Catal. 41 (1996) 253–334.
[30] R. Srivastava, D. Srinivas, P. Ratnasamy, Catal. Lett. 91 (2003) 133.
[31] R. Srivastava, D. Srinivas, P. Ratnasamy, Stud. Surf. Sci. Catal. C 154 (2004) 2703.
[32] R. Srivastava, D. Srinivas, P. Ratnasamy, J. Catal. 233 (2005) 1.
[33] R. Srivastava, D. Srinivas, P. Ratnasamy, Microporous Mesoporous Mater. 90 (2006) 314.
[34] D. Srinivas, R. Srivastava, P. Ratnasamy, Catal. Today 93 (2004) 127.
[35] R. Garro, M.T. Navarro, J. Primo, A. Corma, J. Catal. 233 (2005) 342.
[36] D. Zhao, J. Feng, Q. Huo, N. Melosh, G.H. Fredrickson, B.F. Chmelka, G.D. Stucky, Science 279 (1998) 548.
[37] F. Feng, G.E. Fryxell, L.-Q. Wang, A.Y. Kim, K.M. Kemner, Science 276 (1997) 923.
[38] L. Mercier, T.J. Pinnavaia, Adv. Mater. 9 (1997) 500.
[39] A. Stein, B.J. Melde, R.C. Schroden, Adv. Mater. 12 (2000) 1403.
[40] W.M. Van Rhijn, D.E. De Vos, B.F. Sels, W.D. Bossaert, P.A. Jacobs, Chem. Commun. (1998) 317.
[41] D. Das, J.-F. Lee, S. Cheng, Chem. Commun. (2001) 2178.
[42] E. Cano-Serrano, J.M. Campos-Martin, J.L.G. Fierro, Chem. Commun. (2003) 246.
[43] A. Thangaraj, R. Kumar, P. Ratnasamy, J. Catal. 131 (1991) 294.
[44] D. Margolese, J.A. Melero, S.C. Christiansen, B.F. Chmelka, G.D. Stucky, Chem. Mater. 12 (2000) 2448.
[45] B. Sow, S. Hamoudi, M.H. Zahedi-Niaki, S. Kaliaguine, Microporous Mesoporous Mater. 79 (2005) 129.
[46] R.E. Parker, N.S. Isaacs, Chem. Rev. 59 (1959) 737.